

# Zirconia-Based Sintered Ceramics for Biomedical Applications

Sergey Kulkov<sup>1,2,3,a)</sup> and Svetlana Buyakova<sup>1,2,3,b)</sup>

<sup>1</sup> Institute of Strength Physics and Materials Science SB RAS, Tomsk, 634055 Russia

<sup>2</sup> National Research Tomsk State University, Tomsk, 634050 Russia

<sup>3</sup> National Research Tomsk Polytechnic University, Tomsk, 634050 Russia

<sup>a)</sup> Corresponding author: kulkov@ms.tsc.ru

<sup>b)</sup> sbuyakova@ispms.tsc.ru

**Abstract.** A porous ceramics obtained from ultra-fine powders has been studied. The porosity of ceramic samples was from 15 to 80%. The structure of the ceramic materials was a cellular structure. A distinctive feature of all deformation diagrams obtained in the experiment was their nonlinearity at low deformations which was described by the parabolic law. It was shown that the observed nonlinear elasticity for low deformations on deformation diagrams is due to mechanical instability of the cellular elements in the ceramic carcass.

## INTRODUCTION

Plasma spray synthesis and chemical co-precipitation methods are the main efficient routs for ultra-fine powder production as they activate a sintering process [1]. The sintering process for these powders with identical chemical composition may be very different and final structure of a sintered body depends on a particle size, surface energy strain conserved in the whole system, etc. [2]. For example, one can obtained hollow-ball particles, whose forms will stipulate a special morphology structure of materials [3].

The aim of the work is the investigation of densification, structure and mechanical properties of materials based on zirconia-based powders produced by plasma spray synthesis and sintered at different temperatures.

## MATERIALS AND EXPERIMENTAL PROCEDURE

Ceramic samples made from plasma-sprayed and chemically precipitated (97 mol. %  $ZrO_2$  + 3 mol. %  $Y_2O_3$ ) powders were studied. The ceramic materials used for this study were obtained from powders of  $ZrO_2(MgO)$ , or  $ZrO_2(Y_2O_3)$  (Siberian Enterprise Chemical Group), following chemical co-precipitation, as previously described [4].

To study densification kinetics samples were produced by pressing as-received powders till relative density 0.33 and sintering at 1500°C during 0–20 hours.

Structure investigation was carried out on the samples sintered in the temperature range 1400–1650°C during isothermal holding from 1 up to 5 hours after uniaxial compression with the loading speed  $4 \times 10^{-4} s^{-1}$ .

To determine the exponent of the equation Hollomon [5] ( $\sigma = K\varepsilon^k$ , when  $\sigma$ —true stress;  $\varepsilon$ —true strain;  $k$ —parabolic factor;  $K$ —constant for a given material) experimental data were replotted in “ln-ln” coordinates.

Phase identification and evaluation of coherently diffracted domains (CDD) were determined from X-ray diffractometry data [6, 7]. Scanning electron microscope Philips-SEM 515 and transmission microscope Philips CM 30 were used to determine the structure and average grain and mean size of pores.

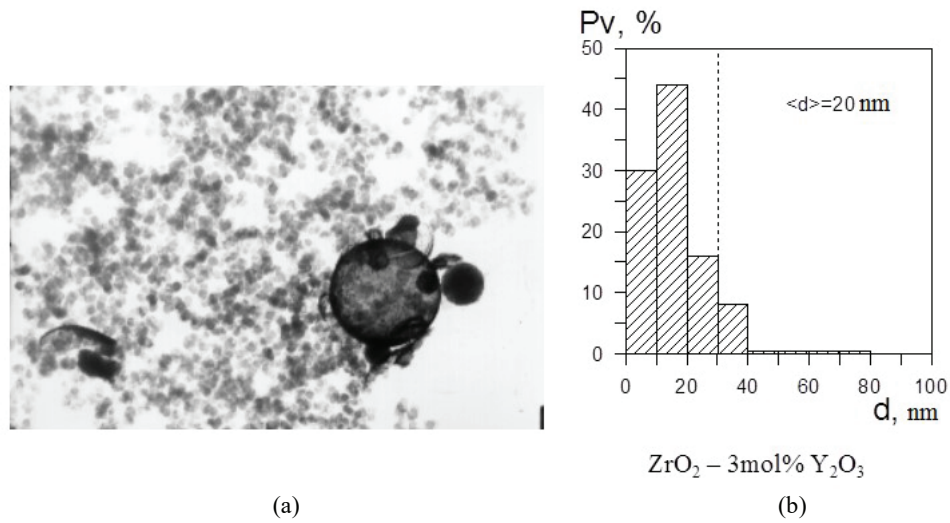


FIGURE 1. TEM image of ZrO<sub>2</sub> powder, synthesized by plasma-sprayed method (a) and grain-size distribution (b)

## RESULTS AND DISCUSSION

Zirconia powder was characterized by spherical particles and their agglomerates (Fig. 1a). An average particle size was 1.5 μm. It was measured that specific surface of chemically precipitated powder was equal to 7 m<sup>2</sup>/g. According to the X-ray data the tetragonal phases of ZrO<sub>2</sub> was predominant in the amount of 95% with an average CDD size 20 nm. An average CDD size of monoclinic phase was equal to 20 nm and the same value was obtained from size distribution in TEM investigations (Fig. 1b). This means that grains are mono-domain crystals.

Density dependences during sintering process are represented in Fig. 2 and one can conclude that most intensive densification occurred at heating stage. The analyzing of this dependence using equation of the form  $\Delta L/L = K\tau^n$ ,  $\Delta L/L$ —relative shrinkage,  $K$ —kinetic coefficient,  $n$ —constant of densification rate, in log-log coordinates, were revealed that  $n$  for the samples made from plasma-sprayed powder is twice as big as for samples based on chemically precipitated powder; 0.1 and 0.04 accordingly [3].

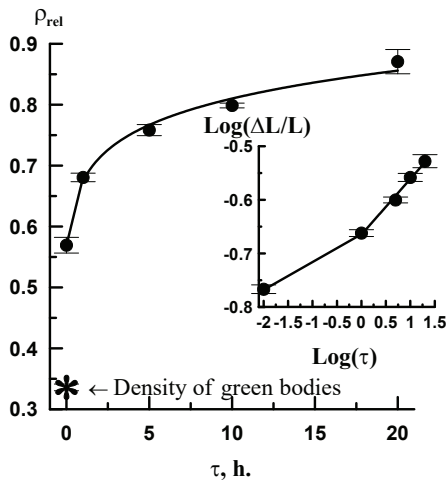


FIGURE 2. Dependences of relative density on the duration of isothermal holding for ZrO<sub>2</sub> powder and kinetic dependences of samples shrinkage during isothermal holding

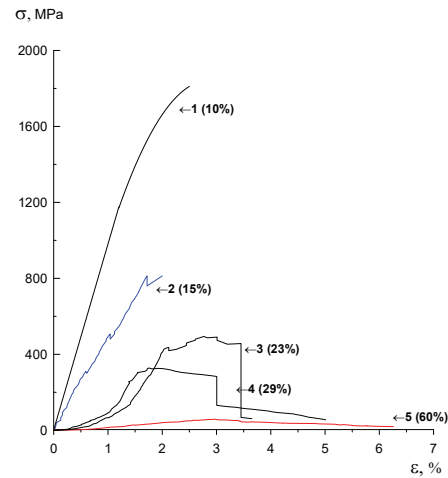
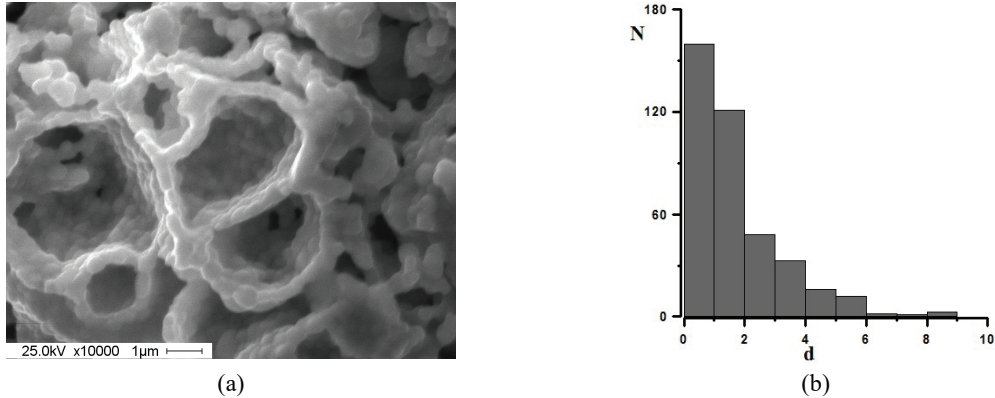


FIGURE 3. Stress-strain diagrams of sintered zirconia with different porous space



**FIGURE 4.** Fracture surface of sintered ceramic samples (a) and pore size distribution for ZrO<sub>2</sub> with 40% porosity (b)

X-ray analysis had shown, that the tetragonal phase content in sintered ceramics was decreasing with increasing of the holding time up to 5 hours for materials based on plasma-sprayed powder from 95 to 60%, further increase of holding time didn't influence the phase composition.

Stress-strain diagram of porous ceramics, which were gained by plasma-sprayed method, are presented in Fig. 3. The obtained stress-strain diagrams had a descending branch with a monotonic decrease of stress. It is an evidence of damages accumulation in the samples in contrast to the stress-strain diagrams of brittle materials with a homogeneous structure.

Microdamages appearing in the material had local nature and the sample under load retained the ability to resist increasing load. A distinctive feature of all the  $\sigma$ - $\varepsilon$  diagrams obtained in the experiment was their nonlinearity at low deformations which was described by the parabolic law. Cyclic loading of samples on parabolic section of diagrams did not reveal residual strain. Therefore, the nonlinearity in the stress-strain diagrams was due to the elastic deformation of ceramics with cellular structure.

The structure of the ceramic materials produced from plasma-sprayed ZrO<sub>2</sub> powder was represented as a system of cell and rod structure elements (Fig. 4). Cellular structure formed by stacking hollow powder particles can be easily seen at the images of fracture surfaces of obtained ceramics. There were three types of pores in ceramics: large cellular hollow spaces, small interparticle pores that are not filled with powder particles and the smallest pores in the shells of cells. The cells generally did not have regular shapes. The size of the interior of the cells many times exceeded the thickness of the walls which was a single-layer packing of ZrO<sub>2</sub> grains. The increase of the pore space in the ceramics was accompanied by the decrease of the average size of voids inside the cells and the average grain size.

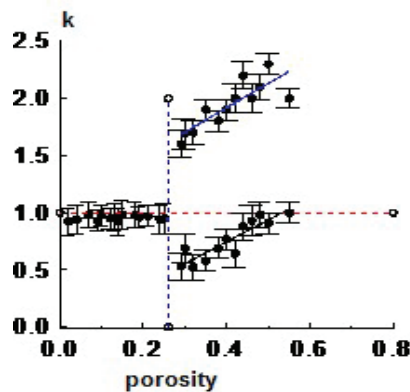


**FIGURE 5.** Parabolic factor of the deformation equation vs. porous space volume of sintered ZrO<sub>2</sub>

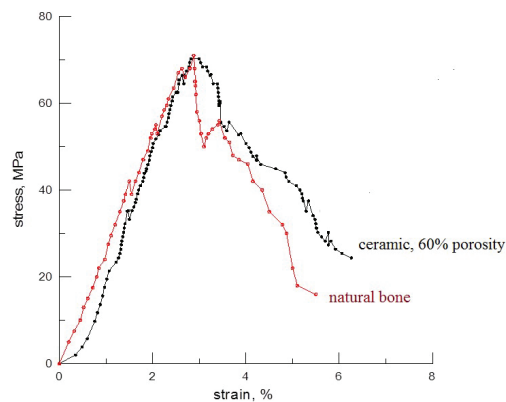


**FIGURE 6.** Stress-strain diagrams of sintered zirconia with 60% porosity as compared with natural bone

Replotting stress-strain diagrams in “ln-ln” coordinates allowed us to determine the exponent of the equation Hollomon [5]  $\sigma = K\varepsilon^k$ , when  $\sigma$ —true stress,  $\varepsilon$ —true strain,  $k$ —parabolic factor from the experimental data. In this case, the index takes the value of the power function of the slope of the strain diagram in logarithmic scale.

Analysis of stress-strain diagrams for ceramics with different porosity reveals that the expansion of the pore space volume in ceramics structure induces multiple microdamage during deformation; in doing so, the higher the porosity, the more pronounced the microdamage. This process is manifested in the diagrams as sharp stress drops due to microcracking. Microcracks are stops by pores and the material restores the capacity for elastic deformation. The region of microcracking manifestation with porosity growth is shifted to the region of high stresses and becomes more extended. The stress-strain diagrams for ceramics with porosity higher than 20% are non-linear, which is absolutely atypical of the loading curves of sintered materials. The slopes in the curves  $\sigma = f(\varepsilon)$  under active loading up to microcracking change depend on the porosity value. Such dependences can be described by a power function of the type both for the process related with deformation and for the process related with compaction of a porous solid, whose manifestation can be expected in the given system. In this case, the value of the exponent  $n$  is defined by which of the processes—compaction or plastic deformation—is the governing one in this material. For purely elastic deformation  $k = 1$ , for plastic deformation  $k < 1$ , and for compaction  $k > 1$ .

Analysis of the dependence  $\sigma = f(\varepsilon)$  in logarithmic coordinates shows that diagrams for ceramics with porosity higher than ~20% transform to several rectilinear portions and correspondingly have several values of  $n$ . The higher the porosity, the larger the number of linear portions that can be distinguished. The experimental values of  $k$  fit well into the three lines (Fig. 5), i.e. there is a critical porosity value at which the deformation pattern of the porous solid changes drastically—a second exponent of the power function arises which is much higher than in the initial state. This is most likely associated with a change in the pore distribution pattern—from isolated pores to continuous porous structure. The material is actually divided into two subsystems deformed in different ways under external loading.

No displacement of material volumes to the pore space has been found experimentally and we may thus assume that no compaction but only elastic deformation, i.e. elastic interaction of elementary volumes in the porous structure, takes place. These data were explained early [3] and it has been shown that in such a system one can observe losses of deformation stability of cell-like or rod-like structures formed in ceramics during sintering. According to these estimates, even at stability loss in rod-shaped structures with a small number of elements they may undergo noticeable macrodeformation in the elastic region as structural elements, which are observed experimentally.

Sintered ceramic with a high porosity obtained in this study has a very similar behavior as compared with natural bone, figure 6. As one can see from the figure a stress-strain diagram of these materials has same peculiarities—microcracking on active loading and damages accumulation after maximum stresses. Therefore, this ceramic can be used as perspective material for bone replacement.

## CONCLUSION

It has been shown that the most intensive densification of studied materials took place during heating stage. In the stress-strain diagrams the nonlinearity occurred due to the elastic deformation of ceramics with cellular structure. The character of the received strain-porosity dependences probably was a result of porosity type change.

It has been shown that the “stress – strain” diagrams on the initial stage of deformation had a nonlinear behavior with high parabolic factor of strain–stress curves. It has been shown that fracture of the materials was observed from the elastic area and has rod-like or cellular-like parts in its structure.

Sintered ceramic with a high porosity has a very similar behavior as compared with natural bone and can be used as perspective material for bone replacement.

## ACKNOWLEDGMENTS

This research has been carried out with the partial financial support of the Ministry of Education and Science of the Russian Federation RFMEFI60714X0069.

The study reported in this article was conducted according to accepted ethical guidelines involving research in humans and/or animals and was approved by an appropriate institution or national research organization. The study is compliant with the ethical standards as currently outlined in the Declaration of Helsinki. All individual partici-

pants discussed in this study, or for whom any identifying information or image has been presented, have freely given their informed written consent for such information and/or image to be included in the published article.

## REFERENCES

1. I. M. Fedorchenko and I. I. Ivanova, About influence of particle size and specific surface on densification during the sintering, in *Theory and Technology of Sintering* (Naukova Dumka, Kiev, 1974), pp. 193–199.
2. A. I. Gusev and A. I. Rempel, *Nanocrystalline Materials* (PHYSMATHLIT, Moscow, 2001).
3. S. N. Kulkov and S. P. Buyakova, Structure, phase composition and technologies features of zirconia-based nanosystems, *Rus. Nanotechnology* **2**(1), 119–132 (2007).
4. E. Kalatur, S. Buyakova, S. Kulkov, and A. Narikovich, Porosity and mechanical properties of zirconium ceramics, *AIP Proceedings* **1623** (Melville, New York, 2014), pp. 225–228.
5. R. W. Hertzberg, *Deformation and Fracture Mechanics of Engineering Materials* (John Wiley and Sons, Inc., 1989).
6. H. Torayda, M. Yoshimura, and S. Somiya, *J. Am. Ceram. Soc.* **67**(6), 119–121 (1984).
7. S. S. Gorelic, Yu. A. Skakov, and L. N. Rastorguev, *X-ray and Electron/Optical Microscope Analysis* (MISIS, Moscow, 1994).